PHYSICAL REVIEW B **94**, 180409(R) (2016)

Controlling Gilbert damping in a YIG film using nonlocal spin currents

M. Haidar,* P. Dürrenfeld, M. Ranjbar, M. Balinsky, M. Fazlali, M. Dvornik, and R. K. Dumas
Department of Physics, University of Gothenburg, 41296 Gothenburg, Sweden

S. Khartsev
Department of Integrated Devices and Circuits, School of ICT, Royal Institute of Technology (KTH), 16440 Kista, Sweden

J. Åkerman
Department of Physics, University of Gothenburg, 41296 Gothenburg, Sweden
and Materials Physics, School of ICT, Royal Institute of Technology (KTH), 16440 Kista, Sweden

(Received 26 December 2015; revised manuscript received 5 November 2016; published 28 November 2016)

We demonstrate the control of Gilbert damping in 65-nm-thick yttrium iron garnet (YIG) films using a spin-polarized current generated by a direct current through a nanocontact, spin filtered by a thin Co layer. The magnetodynamics of both the YIG and the Co layers can be excited by a pulse-modulated microwave current injected through the nanocontact and the response detected as a lock-in amplified voltage over the device. The spectra show three clear peaks, two associated with the ferromagnetic resonance (FMR) in each layer, and an additional Co mode with a higher wave vector proportional to the inverse of the nanocontact diameter. By varying the sign and magnitude of the direct nanocontact current, we can either increase or decrease the linewidth of the YIG FMR peak consistent with additional positive or negative damping being exerted by the nonlocal spin current injected into the YIG film. Our nanocontact approach thus offers an alternative route in the search for auto-oscillations in YIG films.

DOI: 10.1103/PhysRevB.94.180409

Recently, yttrium iron garnet (YIG) thin films have garnered intense interest in spintronics [1–5], and magnonics [6–9]. As YIG has ultralow Gilbert damping, it is an ideal medium for spin waves (SWs) to propagate over long distances (hundreds of microns [10]) which is very desirable for microwave technologies. The Gilbert damping is an intrinsic material parameter and significant efforts have been made to control and tune it, e.g., using spin transfer torque (STT) [11–13], i.e., the transfer of angular momentum between a spin, or a spin-polarized, current and the local magnetization in the film. Depending on the relative orientation of the Gilbert damping torque and the STT, the damping can be either enhanced or reduced. So far, a tunable spin-wave damping in YIG [14–16] has been demonstrated by a pure spin current generated by spin-orbit torque [17–20] using two approaches. First, a spin current can be created electrically using the spin Hall effect by passing a direct current through a heavy metal [1,14,15]. Second, a spin current can be generated thermally via the spin Seebeck effect through a temperature gradient across a gadolinium gallium garnet (GGG)/YIG/heavy metal trilayer [16,21]. Due to its strong spin-orbit coupling, Pt is used in both approaches to generate the spin current. However, it has also been shown that the Gilbert damping of these devices increases drastically by one order of magnitude due to the strong spin-orbit coupling and spin pumping [22]. This has the effect of (1) strongly reducing the propagation length of the spin waves and (2) requiring a higher threshold current to fully compensate the damping and generate auto-oscillation in YIG.

Pure spin currents can also be generated in a nonlocal geometry, e.g., in lateral spin valves [23], where a charge current is spin polarized by a ferromagnetic injection electrode and a pure spin current can diffuse away from the direction of the charge current. It was recently demonstrated that such a spin current in a Co/Cu lateral spin valve can also be modulated by the orientation of the magnetization of a YIG substrate [24]. Very recently, sustained magnetization auto-oscillation in a permalloy thin film was also reported using a nonlocal geometry [25]. As this geometry also lends itself to injection of a nonlocal pure spin current into an insulator, it could potentially allow for sustained magnetization auto-oscillation in YIG films and the generation of localized [26,27] and propagating [27–29] spin-wave modes as in all-metal nanocontact spin torque oscillators. Here, we investigate this possibility and demonstrate current control of the Gilbert damping in YIG films using nonlocal nanocontact devices.

Our devices are based on pseudospin valves made from a GGG/YIG(65)/Ag(6)/Co(8)/Cu(3)/Pd(3) thin-film stack (thicknesses in nanometers), as shown in Fig. 1(a). The YIG film used in this study was grown using pulsed laser deposition (PLD) [30] and the other layers were deposited *ex situ* using magnetron sputtering after an additional wet cleaning of the YIG surface [31,32]. In the pseudospin valve, Co is the spin-polarizing layer and the YIG film serves as the free layer.

We first studied the impact of Ag and Ag/Co on the magnetodynamics of YIG using ferromagnetic resonance (FMR) measurements by comparing the properties of YIG(65), YIG(65)/Ag(6), and YIG(65)/Ag(6)/Co(8) films. The FMR measurements were carried out using a NanOsc Instrument PhaseFMR system with an in-plane field (H_{ext}) and a coplanar waveguide where the FMR response is measured at different frequencies (f) over the range of 3–14 GHz. We extracted the effective magnetization ($4\pi M_{eff}$) of YIG to be (2313 ± 13) G.

*mohammad.haidar@hotmail.fr

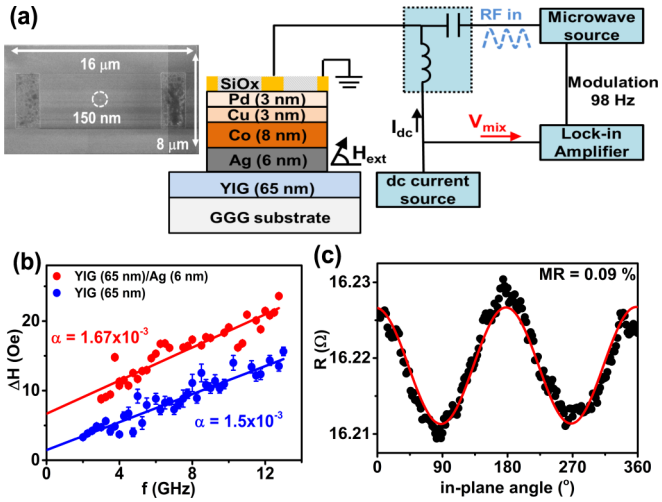

FIG. 1. (a) Sketch of the spin valve stack consisting of YIG/Ag/Co and the circuit used for the ST-FMR measurements. (b) Variation of the FMR linewidth as a function of the frequency for YIG (blue) and YIG/Ag bilayer (red). (c) MR measurements as a function of the in-plane applied field angle θ, measured under an external field $H_{\text{ext}} = 1000$ Oe.

Figure 1(b) then shows the variation of the linewidth (ΔH) as a function of the frequency. The Gilbert damping (α) is extracted from ΔH using the relation $\Delta H = \frac{2\alpha}{\gamma}(2\pi f) + \Delta H_0$, where $\gamma/2\pi$ is the gyromagnetic ratio and ΔH_0 is the inhomogeneous broadening. The extracted magnetodynamics parameters of the films are summarized in Table I.

The slight increase in the Gilbert damping at the YIG/Ag interface is due to weak spin pumping [2]. Contrary to YIG/Pt devices, where the Gilbert damping increases dramatically compared to that of the bare YIG film, in our devices the damping of the YIG film changes only slightly. The enhancement of ΔH_0 could be due to surface roughness at the YIG interface as the Ag/Co layers are *ex situ* deposited as well as due to nonuniformities introduced through nanofabrication. The effective spin-mixing conductance ($g^{\uparrow\downarrow}$) at the YIG interface is calculated using $g^{\uparrow\downarrow} = \frac{4\pi M_s t}{\gamma h}(\alpha_{\text{YIG/Ag/Co}} - \alpha_{\text{YIG}})$, where t and h are the thickness of YIG and Planck's constant, respectively. The extracted effective spin-mixing conductance (Table I) is similar to literature values of YIG/NM (normal metal) [33,34].

To fabricate devices, the Ag and Co layers are patterned into a mesa of 8×16 μm^2 using ion milling, leaving the YIG film fully extended. On top of the mesa, a nominally 150-nm-diameter circular nanocontact is fabricated by means of electron-beam lithography. Figure 1(c) shows the magnetoresistance (MR) of the device—that is, the change in the resistance with an in-plane rotation of the magnetic field with a fixed magnitude of 1000 Oe. It shows an MR ratio of 0.09%. Figure 1(a) depicts the circuit used for the spin-transfer-driven ferromagnetic resonance (ST-FMR) measurements [35–38]. The devices are connected to a pulse-modulated signal generator to excite the dynamics in the spin valve and to a lock-in amplifier to detect the mixing voltage. The devices are placed in a uniform magnetic field where the measurements were performed by sweeping the magnetic field at a fixed frequency, which minimizes the nonmagnetic background response of the measurement circuit. The measurements were performed over a broad range of the frequency (4–25 GHz) with an input power $P = 0$ dBm and at room temperature.

TABLE I. Properties of the different YIG film stacks.

Samples	$4\pi M_{\text{eff}}$ (G)	α (10^{-3})	ΔH_0 (Oe)	$g^{\uparrow\downarrow}$ (10^{18} m^{-2})	Roughness (nm)
YIG	2313 ± 13	1.5	0.92		0.3 ± 0.02
YIG/Ag	2350 ± 20	1.67	6.68	1.31	
YIG/Ag/Co	2284 ± 21	1.71	6.17	1.6	
Device 1	2504 ± 20	1.6	15.1		0.9 ± 0.05
Device 2	2614 ± 20	1.76	10.56	2.35	0.9 ± 0.05

First, we will discuss the ST-FMR spectra measured in the absence of a direct current with a magnetic field oriented in plane. Figure 2(a) shows a typical ST-FMR spectrum measured at $f = 13$ GHz. We can clearly resolve three well-separated peaks. The ST-FMR spectra were fitted with a multipeak Lorentzian function with both symmetric and antisymmetric components [35,38]. From the fit, the resonance field (H) and linewidth ΔH are extracted. Following the resonance frequency as a function of the resonance field for the prominent peaks, the YIG (blue dots) and Co (red dots) can be distinguished, as shown in Fig. 2(b). The effective magnetization (M_{eff}) is extracted using the Kittel equation, $f = \frac{\gamma}{2\pi}\sqrt{H(H + 4\pi M_{\text{eff}})}$. We measure $4\pi M_{\text{eff}} = (2504 \pm 12)$ G and $(13\,435 \pm 200)$ G for YIG and Co, respectively. While the tabulated bulk value of the saturation magnetization for YIG is $4\pi M_s = 1760$ G, a similar increase in M_{eff} of the PLD-grown YIG has been reported and attributed to a strong uniaxial anisotropy caused by Fe^{3+} vacancies within octahedral sites [39]. The third mode (violet dots) corresponds to a resonance excited by the nanocontact. The nanocontact acts as an antenna that generates excitations with a finite wave vector (k) that is inversely proportional to its diameter [40]. The third mode is well fit with the exchange dominated spin-wave dispersion relation, $f = \frac{\gamma}{2\pi}\sqrt{(H + \frac{2A}{\mu_0 M_s}k^2)(H + \frac{2A}{\mu_0 M_s}k^2 + 4\pi M_{\text{eff}})}$, where A is the exchange constant. Using the parameters of Co with $A = 27$ pJ/m, we find that this mode corresponds to a spin-wave mode excited at $k = 25.1$ μm^{-1}. Figure 2(c) shows the variation in ΔH as a function of the frequency of the YIG and Co peaks. For YIG, the measurements were performed on two similar devices. We extract the Gilbert damping of YIG and Co from the slope of the linear fit (lines). We find a slight device-to-device variability in α_{YIG} as indicated in Table I, and $\alpha_{\text{Co}} = (11 \pm 1) \times 10^{-3}$ in addition to a large ΔH_0 for YIG and Co, which may be attributed to mode degeneracy [41].

Second, we investigated the effects of a dc current on the magnetodynamics of YIG. Figure 3 shows results of the measurements performed with an applied dc current I between +5 and −5 mA of the YIG resonance at different frequencies (6–20 GHz) on two similar devices. It shows the variation of the linewidths as a function of the dc current. A change in ΔH with I—depending on the current polarity—can be seen. For the negative (positive) polarity, ΔH decreases (increases) with an increase in $|I|$. This observation is well accounted within the context of spin transfer torque, where a spin-polarized

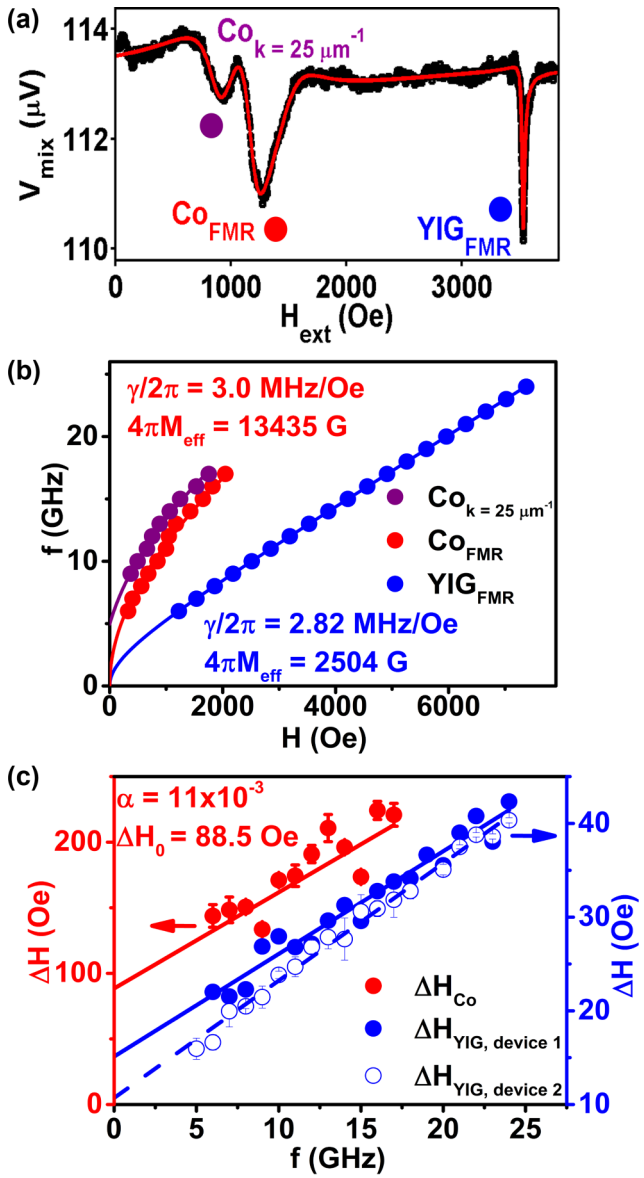

FIG. 2. ST-FMR results at $I = 0$ mA. (a) A typical ST-FMR spectrum (black circles) measured at $f = 13$ GHz showing peaks of YIG, Co, and a third mode. The solid red line is a Lorentzian fit. (b) Field dependence of the resonance frequency of YIG (blue dots), Co (red dots), and the third mode (violet dots) in the ST-FMR spectra. (c) Variation of the linewidth as a function of frequency for YIG and Co. Lines are linear fits.

current will modify the damping, and consequently ΔH, of the YIG layer in a spin valve. According to this model, the spin transfer torque is aligned collinearly to the Gilbert damping torque. For this reason, the spin torque can act to enhance or reduce the effective damping. The variation of the resonance field with the dc current is negligible, which indicates that the heat associated with I has an insignificant impact on the measurements. According to Refs. [42,43], the measured ΔH can be expressed as

$$\Delta H = \frac{2\pi f}{\gamma} 2\alpha + \Delta H_0 + \frac{2\pi f}{\gamma(H + 2\pi M_{\text{eff}})} \frac{\cos(\theta)}{4\pi M_s t} \frac{\hbar J_s}{2e}, \quad (1)$$

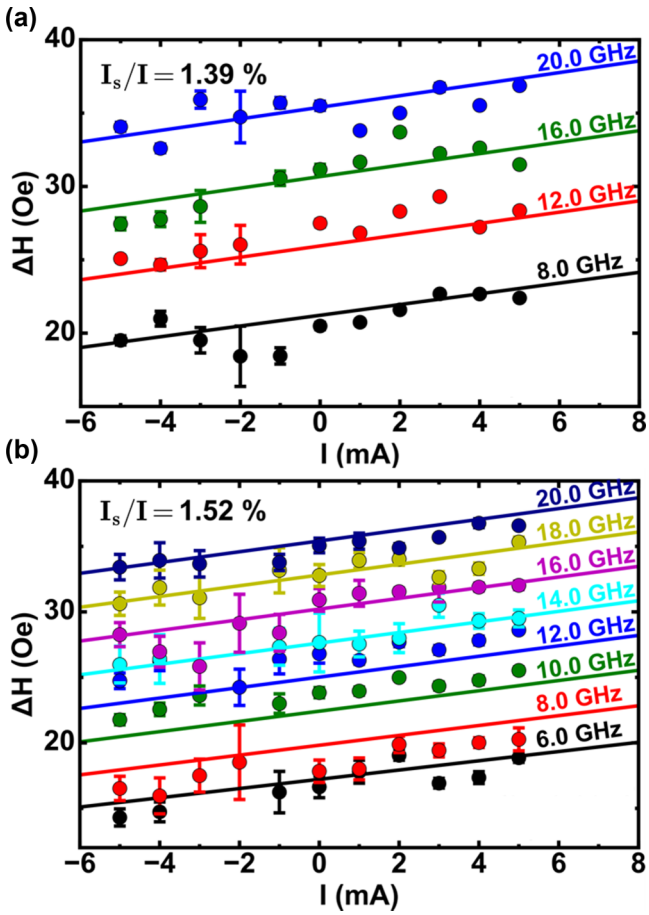

FIG. 3. ST-FMR results in the presence of a dc current. Variation in the linewidth of YIG as a function of the dc current at different frequencies for (a) device 1 and (b) device 2.

where e is the charge of the electron. The third term on the right-hand side describes the additional damping term induced by the spin current density (J_s) on the magnetization of YIG. The solid lines in Fig. 3 are linear fits of ΔH to Eq. (1) [44]. Hence we can express $\Delta H(I)$ as $\Delta H(I = 0\ \text{mA}) + \beta \times I$, where β is a constant representing the change in ΔH due to the current and it is equal to $\frac{2\pi f}{\gamma(H+2\pi M_{\text{eff}})} \frac{\cos(\theta)}{4\pi M_s t} \frac{\hbar}{2e} \frac{P}{A_{\text{NC}}}$, where P is the degree of the spin polarization and A_{NC} is the area of the nanocontact. We found β to be frequency independent with an average value of (0.38 ± 0.07) Oe/mA. This is justified since the dampinglike torque is proportional to $\frac{f}{\gamma(H+2\pi M_{\text{eff}})}$ that results in a frequency-independent behavior of β. Thus the current-induced damping is added to the inhomogeneous broadening. The injected J_s into the YIG film is equal to an average value of 1.45% of the applied current density, which is somewhat lower than that injected in YIG/Pt devices.

Finally, we discuss the ST-FMR measurements that were performed at $f = 8$ GHz with an external field angle tilted out of plane. First, we observe that the resonance field increases with the field angle from 1858 Oe at 0° to 5688 Oe at 90°. The variation in the resonance field is due to the change in the sample demagnetization field. Figure 4(a) shows the changes in the linewidth as a function of the field angle for $I = 0$ mA. A typical behavior of thin films can be seen [45,46]. For

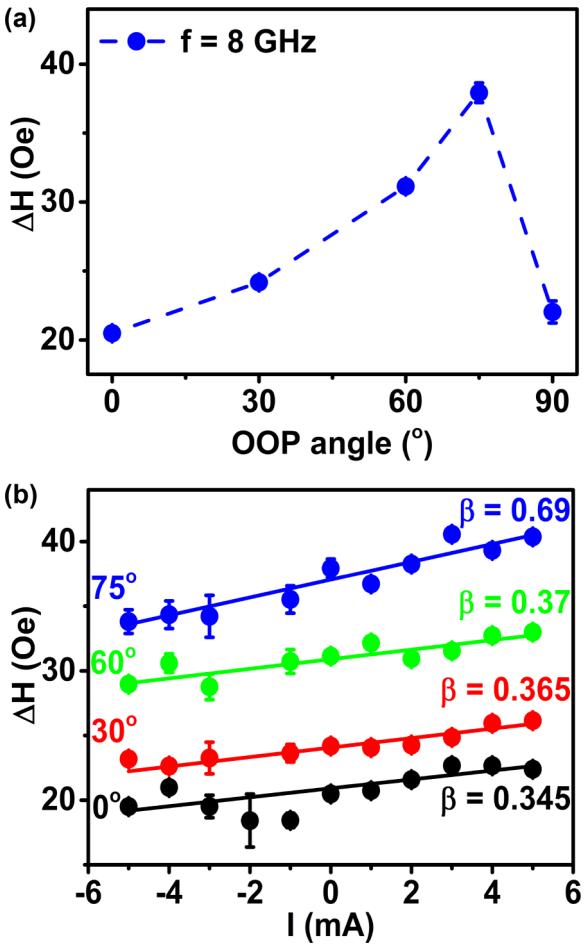

FIG. 4. Angular dependence of the linewidth of YIG measured at $f = 8$ GHz on device 1 (a) at $I = 0$ mA and (b) as a function of the dc current.

in-plane fields, the linewidth increases slowly, until it reaches a significant peak, and then decreases at angles close to the out-of-plane configuration. The difference in the linewidth for the in-plane and out-of-plane measurements is relatively small, which indicates that the two-magnon scattering mechanism is relatively inactive in the sample [47]. The peak around 75° is due to a difference between the field angle and the magnetization angle as the field is rotated to an oblique angle.

In the presence of a dc current, the linewidth increases at $+I$ and decreases at $-I$ for the overall angular dependence—and not only at the in-plane angle, confirming the expectation of STT, as shown in Fig. 4(b) [48]. By extracting the slope from a linear fit at each angle, we can see that β depends on the field angle. We measured an increase in β from 0.34 Oe/mA at the in-plane field to 0.69 Oe/mA at 75°. This is justified in the context of STT theory, since the spin torque [49] depends on the relative orientation of the magnetization of the free layer and the spin-polarized electrons—that is, on the direction of the polarizer layer. For large misalignments between the magnetization of the fixed and the free layers (such as for 75°), the exerted spin torque is expected to be larger.

In conclusion, we have demonstrated the feasibility of controlling the linewidth of spin-wave resonance in YIG electronically by fabricating a YIG-based spin valve. By using the ST-FMR technique, we achieved a direct measurement of the damping of YIG and showed its tunability with the applied direct current. These results will be promising for the fields of YIG-based magnonics and spintronics. The proposed spin valve could be further improved and used to drive persistent oscillations in a confined YIG nanostructure, as such confinement will certainly quantize the spin wave modes.

We thank Afshin Houshang for help with the AFM measurements. This work was supported by the Swedish Foundation for Strategic Research (SSF), the Swedish Research Council (VR), and the Knut and Alice Wallenberg foundation (KAW). This work was also supported by the European Research Council (ERC) under the European Community's Seventh Framework Programme (FP/2007-2013)/ERC Grant No. 307144 "MUSTANG." M.D. would like to thank the Wenner-Gren Foundation for the provided financial support.

[1] Y. Y. Kajiwara, K. Harii, S. Takahashi, J. Ohe, K. Uchida, M. Mizuguchi, H. Umezawa, H. Kawai, K. Ando, K. Takanashi, S. Maekawa, and E. Saitoh, Nature (London) **464**, 262 (2010).

[2] B. Heinrich, C. Burrowes, E. Montoya, B. Kardasz, E. Girt, Y.-Y. Song, Y. Sun, and M. Wu, Phys. Rev. Lett. **107**, 066604 (2011).

[3] T. Chiba, G. E. W. Bauer, and S. Takahashi, Phys. Rev. Appl. **2**, 034003 (2014).

[4] M. B. Jungfleisch, W. Zhang, J. Sklenar, J. Ding, W. Jiang, H. Chang, F. Y. Fradin, J. E. Pearson, J. B. Ketterson, V. Novosad, M. Wu, and A. Hoffmann, Phys. Rev. Lett. **116**, 057601 (2016).

[5] M. Balinsky, M. Haidar, M. Ranjbar, P. Dürrenfeld, A. Houshang, A. Slavin, and J. Åkerman, IEEE Magn. Lett. **7**, 3101704 (2016).

[6] V. V. Kruglyak, S. O. Demokritov, and D. Grundler, J. Phys. D: Appl. Phys. **43**, 264001 (2010).

[7] A. A. Serga, A. V. Chumak, and B. Hillebrands, J. Phys. D: Appl. Phys. **43**, 264002 (2010).

[8] A. Khitun, M. V. Bao, and K. L. Wang, J. Phys. D: Appl. Phys. **43**, 264005 (2010).

[9] A. V. Chumak, A. A. Serga, and B. Hillebrands, Nat. Commun. **5**, 4700 (2014).

[10] H. Yu, O. d'Allivy Kelly, V. Cros, R. Bernard, P. Bortolotti, A. Anane, F. Brandl, R. Huber, I. Stasinopoulos, and D. Grundler, Sci. Rep. **4**, 6848 (2014).

[11] L. Berger, Phys. Rev. B **54**, 9353 (1996).

[12] J. Slonczewski, J. Magn. Magn. Mater. **159**, L1 (1996).

[13] D. C. Ralph and M. Stiles, J. Magn. Magn. Mater. **320**, 1190 (2008).

[14] A. Hamadeh, O. d'Allivy Kelly, C. Hahn, H. Meley, R. Bernard, A. H. Molpeceres, V. V. Naletov, M. Viret, A. Anane, V. Cros, S. O. Demokritov, J. L. Prieto, M. Muñoz, G. de Loubens, and O. Klein, Phys. Rev. Lett. **113**, 197203 (2014).

[15] M. Collet, X. de Milly, O. d'Allivy Kelly, V. V. Naletov, R. Bernard, P. Bortolotti, V. E. Demidov, S. O. Demokritov, J. L. Prieto, M. Muñoz, V. Cros, A. Anane, G. de Loubens, and O. Klein, Nat. Commun. **7**, 10377 (2016).

[16] L. Lu, Y. Sun, M. Jantz, and M. Wu, Phys. Rev. Lett. **108**, 257202 (2012).

[17] V. E. Demidov, S. Urazhdin, H. Ulrichs, V. Tiberkevich, A. Slavin, D. Baither, G. Schmitz, and S. O. Demokritov, Nat. Mater. **11**, 1028 (2012).

[18] M. Ranjbar, P. Dürrenfeld, M. Haidar, E. Iacocca, M. Balinskiy, T. Q. Le, M. Fazlali, A. Houshang, A. Awad, R. Dumas, and J. Åkerman, IEEE Magn. Lett. **5**, 3000504 (2014).

[19] L. Liu, C.-F. Pai, Y. Li, H. W. Tseng, D. C. Ralph, and R. A. Buhrman, Science **336**, 555 (2012).

[20] V. E. Demidov, S. Urazhdin, E. R. J. Edwards, M. D. Stiles, R. D. McMichael, and S. O. Demokritov, Phys. Rev. Lett. **107**, 107204 (2011).

[21] N. Vlietstra, J. Shan, B. J. van Wees, M. Isasa, F. Casanova, and J. Ben Youssef, Phys. Rev. B **90**, 174436 (2014).

[22] Y. Sun, H. Chang, M. Kabatek, Y.-Y. Song, Z. Wang, M. Jantz, W. Schneider, M. Wu, E. Montoya, B. Kardasz, B. Heinrich, S. G. E. te Velthuis, H. Schultheiss, and A. Hoffmann, Phys. Rev. Lett. **111**, 106601 (2013).

[23] F. Jedema, A. T. Filip, and B. J. van Wees, Nature (London) **410**, 345 (2001).

[24] E. Villamor, M. Isasa, S. Vélez, A. Bedoya-Pinto, P. Vavassori, L. E. Hueso, F. S. Bergeret, and F. Casanova, Phys. Rev. B **91**, 020403 (2015).

[25] V. E. Demidov, A. Urazhdin, A. V. Sadovnikov, A. N. Slavin, and S. Demokritov, Sci. Rep. **5**, 8578 (2015).

[26] V. E. Demidov, S. Urazhdin, and S. O. Demokritov, Nat. Mater. **9**, 984 (2010).

[27] S. Bonetti, V. Puliafito, G. Consolo, V. S. Tiberkevich, A. N. Slavin, and J. Åkerman, Phys. Rev. B **85**, 174427 (2012).

[28] M. Madami, S. Bonetti, G. Consolo, S. Tacchi, G. Carlotti, G. Gubbiotti, F. B. Mancoff, M. A. Yar, and J. Åkerman, Nat. Nanotechnol. **6**, 635 (2011).

[29] R. K. Dumas, E. Iacocca, S. Bonetti, S. R. Sani, S. M. Mohseni, A. Eklund, J. Persson, O. Heinonen, and J. Åkerman, Phys. Rev. Lett. **110**, 257202 (2013).

[30] M. Haidar, M. Ranjbar, M. Balinsky, R. K. Dumas, S. Khartsev, and J. Åkerman, J. Appl. Phys. **117**, 17D119 (2015).

[31] M. B. Jungfleisch, V. Lauer, R. Neb, A. V. Chumak, and B. Hillebrands, Appl. Phys. Lett. **103**, 022411 (2013).

[32] M. Balinsky, M. Ranjbar, M. Haidar, P. Dürrenfeld, R. K. Dumas, S. Khartsev, A. Slavin, and J. Åkerman, IEEE Magn. Lett. **6**, 3000604 (2015).

[33] H. L. Wang, C. H. Du, Y. Pu, R. Adur, P. C. Hammel, and F. Y. Yang, Phys. Rev. Lett. **112**, 197201 (2014).

[34] H. Wang, C. Du, P. Chris Hammel, and F. Yang, Appl. Phys. Lett. **104**, 202405 (2014).

[35] A. A. Tulapurkar, Y. Suzuki, A. Fukushima, H. Kubota, H. Maehara, K. Tsunekawa, D. D. Djayaprawira, N. Watanabe, and S. Yuasa, Nature (London) **438**, 339 (2005).

[36] J. C. Sankey, P. M. Braganca, A. G. F. Garcia, I. N. Krivorotov, R. A. Buhrman, and D. C. Ralph, Phys. Rev. Lett. **96**, 227601 (2006).

[37] H. Kubota, A. Fukushima, K. Yakushiji, T. Nagahama, S. Yuasa, K. Ando, H. Maehara, Y. Nagamine, K. Tsunekawa, D. D. Djayaprawira, N. Watanabe, and Y. Suzuki, Nat. Phys. **4**, 37 (2008).

[38] T. Staudacher and M. Tsoi, J. Appl. Phys. **109**, 07C912 (2011).

[39] S. A. Manuilov, S. I. Khartsev, and A. M. Grishin, J. Appl. Phys. **106**, 123917 (2009).

[40] M. Fazlali, M. Dvornik, E. Iacocca, P. Dürrenfeld, M. Haidar, J. Åkerman, and R. K. Dumas, Phys. Rev. B **93**, 134427 (2016).

[41] R. D. McMichael, D. J. Twisselmann, and A. Kunz, Phys. Rev. Lett. **90**, 227601 (2003).

[42] L. Liu, T. Moriyama, D. C. Ralph, and R. A. Buhrman, Phys. Rev. Lett. **106**, 036601 (2011).

[43] S. Petit, C. Baraduc, C. Thirion, U. Ebels, Y. Liu, M. Li, P. Wang, and B. Dieny, Phys. Rev. Lett. **98**, 077203 (2007).

[44] We perform fits of ΔH vs I and f simultaneously using two methods: (1) Letting the parameters in Eq. (1) free to extract α, ΔH_0, and J_s independently and (2) fixing α and ΔH_0 at their $I = 0$ values and extract J_s. The two methods give almost the same percentage of the injected spin current into YIG.

[45] M. J. Hurben and C. E. Patton, J. Appl. Phys. **83**, 4344 (1998).

[46] J. Dubowik, K. Załęski, H. Głowiński, and I. Gościańska, Phys. Rev. B **84**, 184438 (2011).

[47] M. Sparks, R. Loudon, and C. Kittel, Phys. Rev. **122**, 791 (1961).

[48] The signal at $I = -2$ mA could not be resolved clearly at certain angles.

[49] J_s, which appears in Eq. (1), in a magnetic multilayer is expressed as $J \times g(\theta)$ [12], where $g(\theta)$ is a function that describes the degree of the polarization of the current at the Ag/YIG interface and depends on the angle between the magnetization of Co and YIG layers.